

The multiphase structural evolution and electromagnetic properties driven by Co (III) ions of $\text{La}_{2-x}\text{Sr}_x\text{CoMnO}_6$ ($x = 0\sim 1.0$) polycrystals

Xuesong Wang, Hongyuan Song*, Kun Dong, Ruihang Yao, Haorong Wu, Xiaolong Yang, Liangwei Chen, Bin Liu,
Zhenhua Ge, Lan Yu**

*Faculty of Materials Science and Engineering, Kunming University of Science and Technology, Kunming, 650093,
PR China*

* *Corresponding Authors: songhongyuan0227@outlook.com (Hongyuan Song), yulan000@hotmail.com (Lan Yu).*

The standard crystal structure cif card used for XRD structural refinement is as follows:

Monoclinic crystal system of ordered phase $\text{La}_2\text{CoMnO}_6$ ($P2_1/n$, ICSD #98240);

Orthorhombic crystal system of disordered phase $\text{La}_2\text{CoMnO}_6$ ($Pbnm$, ICSD #151836);

Rhombohedral crystal system of $\text{La}_{1.6}\text{Sr}_{0.4}\text{CoMnO}_6$ ($R3c$, ICSD #151839);

Cubic crystal system of LaSrCoMnO_6 ($Fm-3m$, ICSD # 96530).

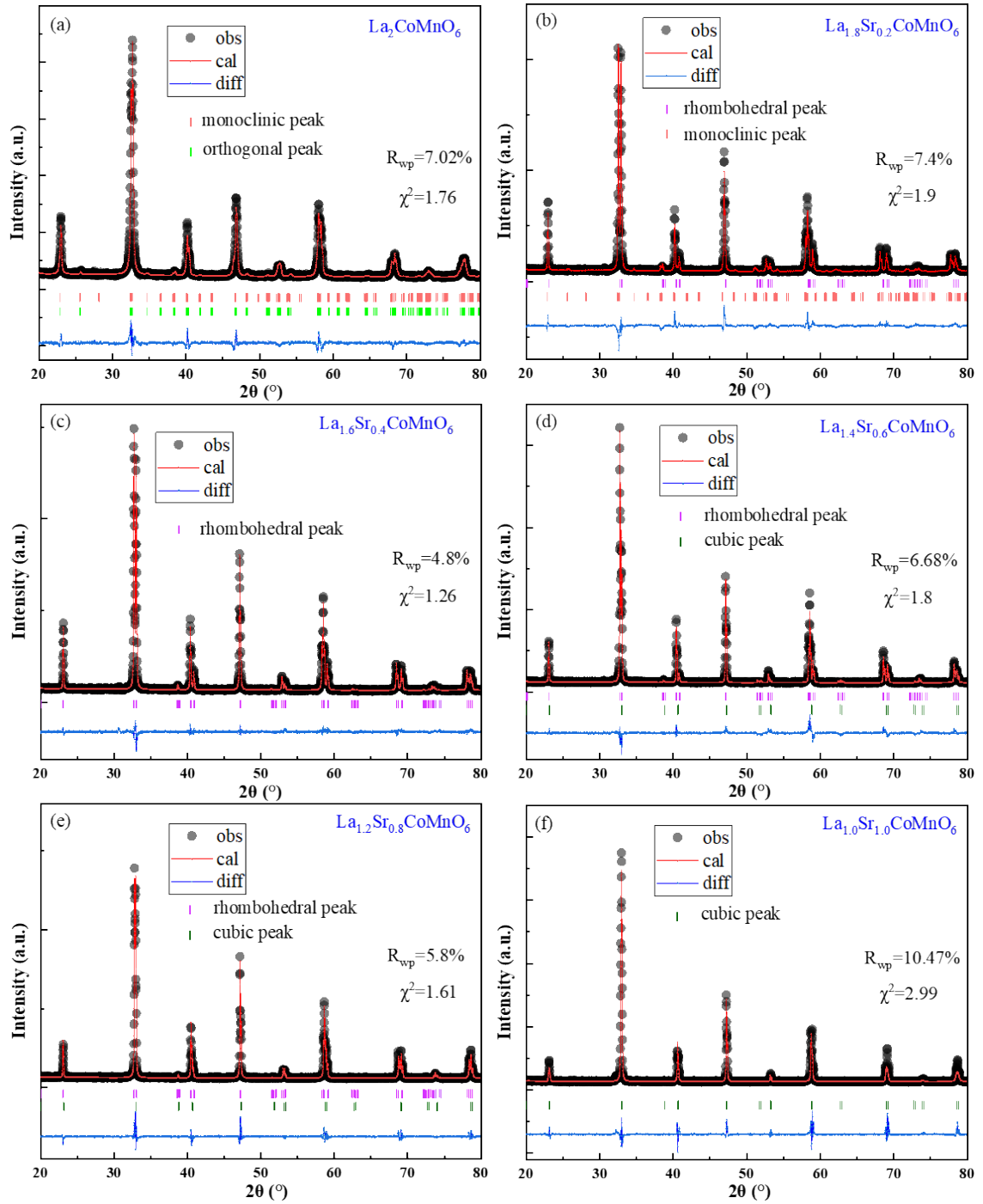


Fig. S1. XRD structural refinement profiles of $\text{La}_{2-x}\text{Sr}_x\text{CoMnO}_6$ ceramics (a) $x = 0$, (b) $x = 0.2$, (c) $x = 0.4$, (d) $x = 0.6$, (e) $x = 0.8$, (f) $x = 1.0$.

Tab. S1. Oxidation states, coordination numbers, and corresponding ionic radii of the elements r_c .

Element	Oxidation	Coordination Number	$r_c/\text{\AA}$
La	+3	XII	1.36
Sr	+2	XII	1.44
Co	+2	VI	0.745
	+3	VI	0.61
Mn	+3	VI	0.654
	+4	VI	0.53
O	-2	VI	1.4

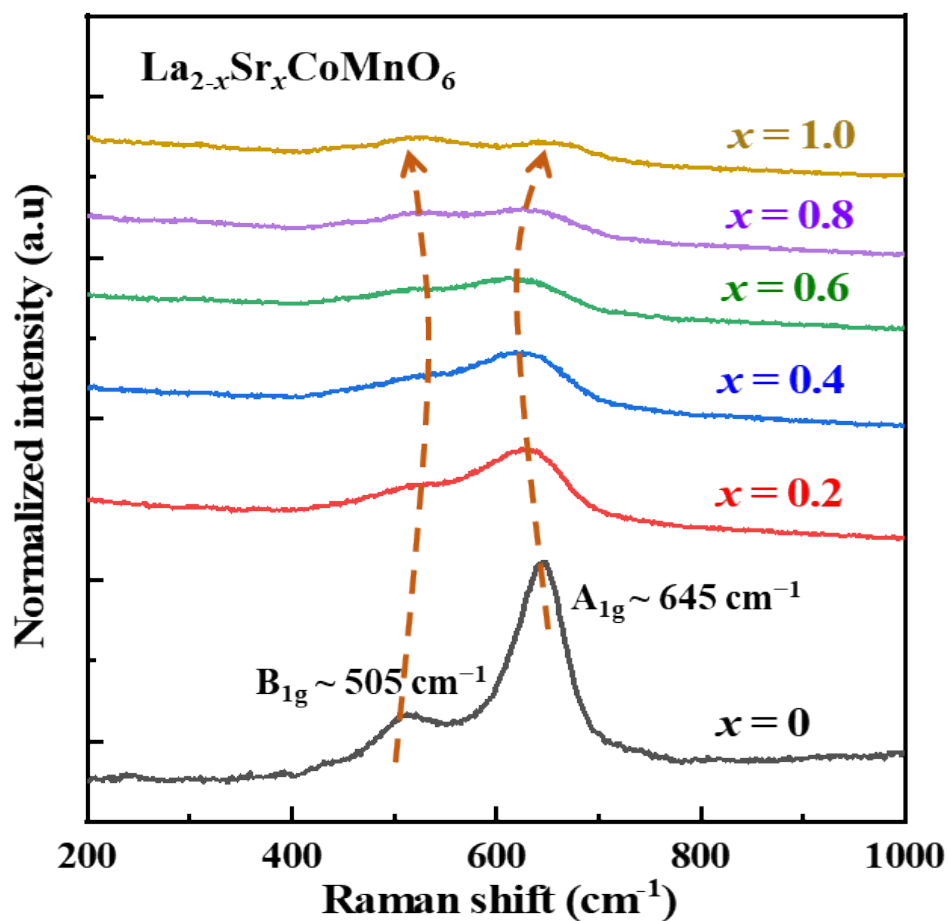


Fig. S2. Raman spectra of $\text{La}_{2-x}\text{Sr}_x\text{CoMnO}_6$ ($x = 0\sim 1.0$) ceramics.

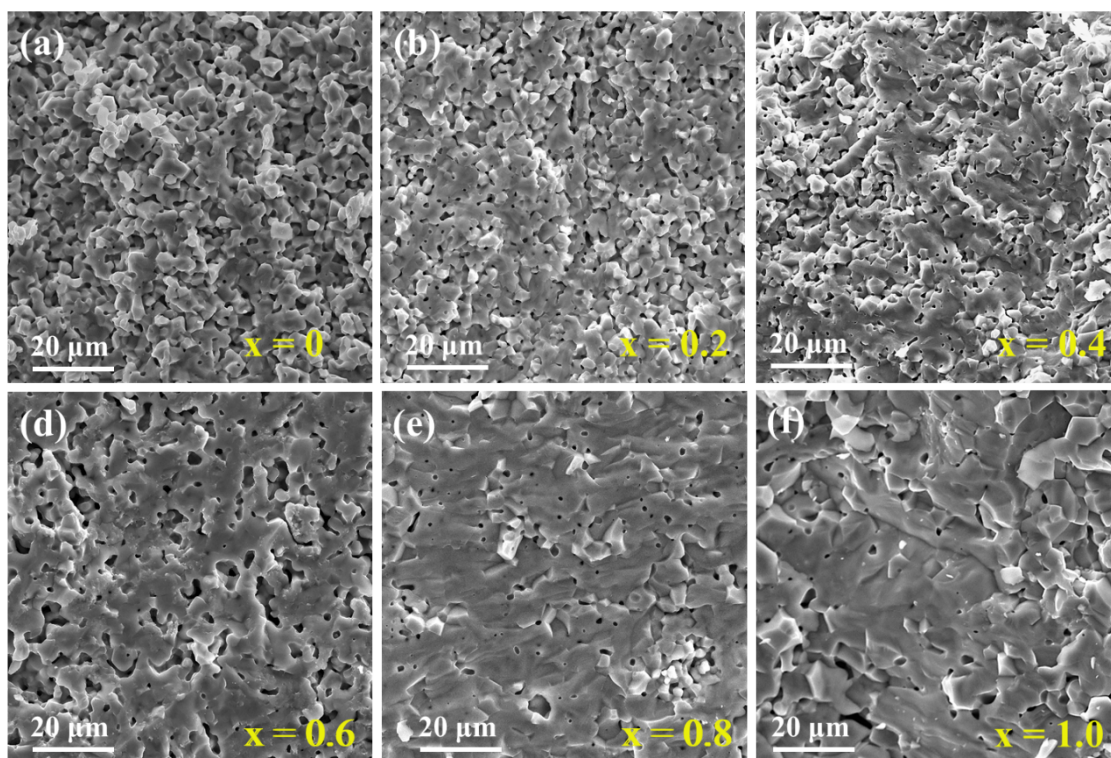


Fig. S3. SEM topography of $\text{La}_{2-x}\text{Sr}_x\text{CoMnO}_6$ ceramics

(a) $x = 0$, (b) $x = 0.2$, (c) $x = 0.4$, (d) $x = 0.6$, (e) $x = 0.8$, (f) $x = 1.0$.

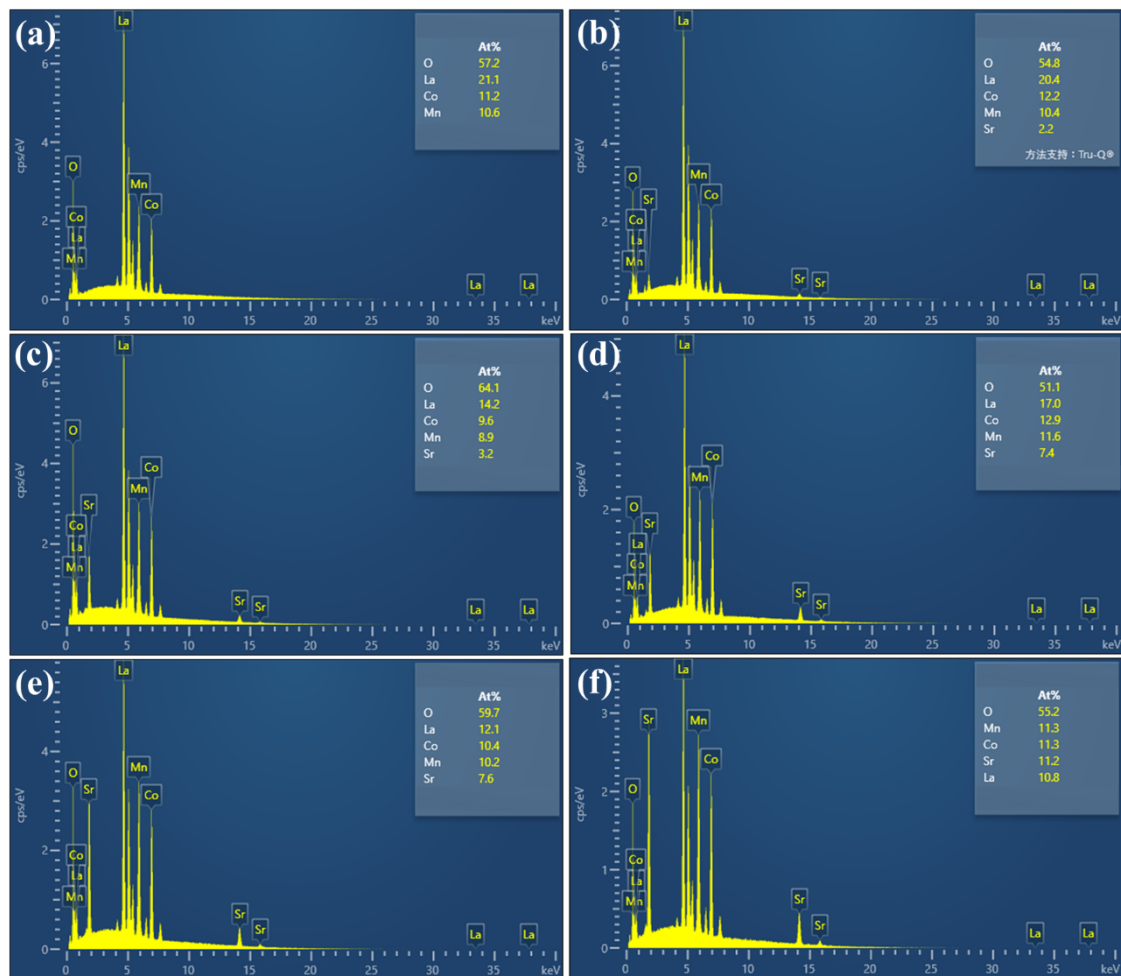


Fig. S4. Atomic ratio of element distribution in EDS atlas of $\text{La}_{2-x}\text{Sr}_x\text{CoMnO}_6$ ceramics (At%) (a) $x = 0$, (b) $x = 0.2$, (c) $x = 0.4$, (d) $x = 0.6$, (e) $x = 0.8$, (f) $x = 1.0$.

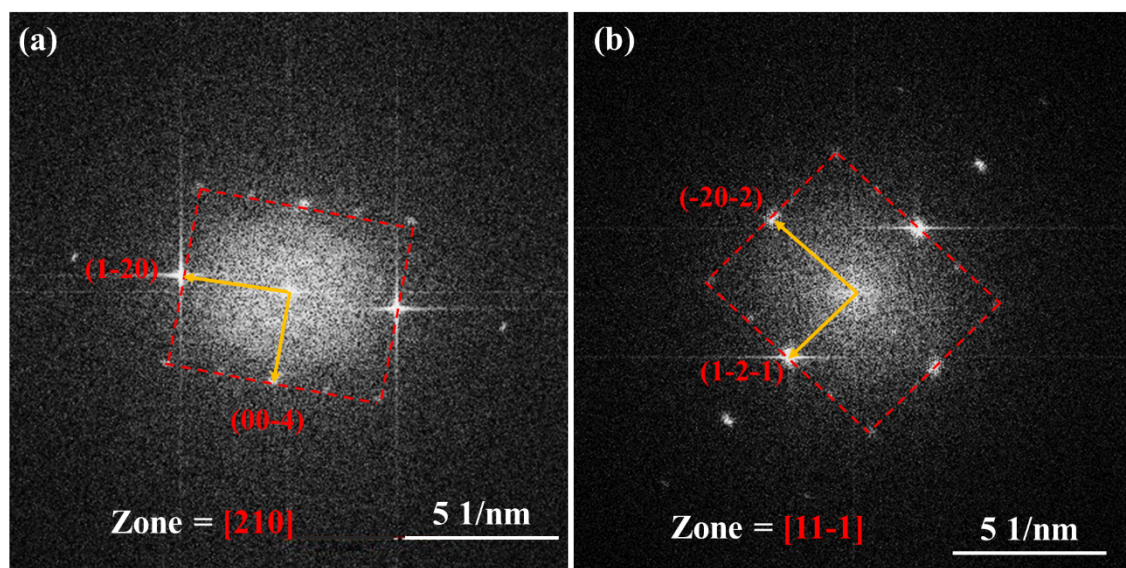


Fig. S5. (a) FFT diagram corresponding to LS0.4CMO along the crystal band axis $[210]$; (b) corresponding to LSCMO FFT diagram along the $[11-1]$ band axis.

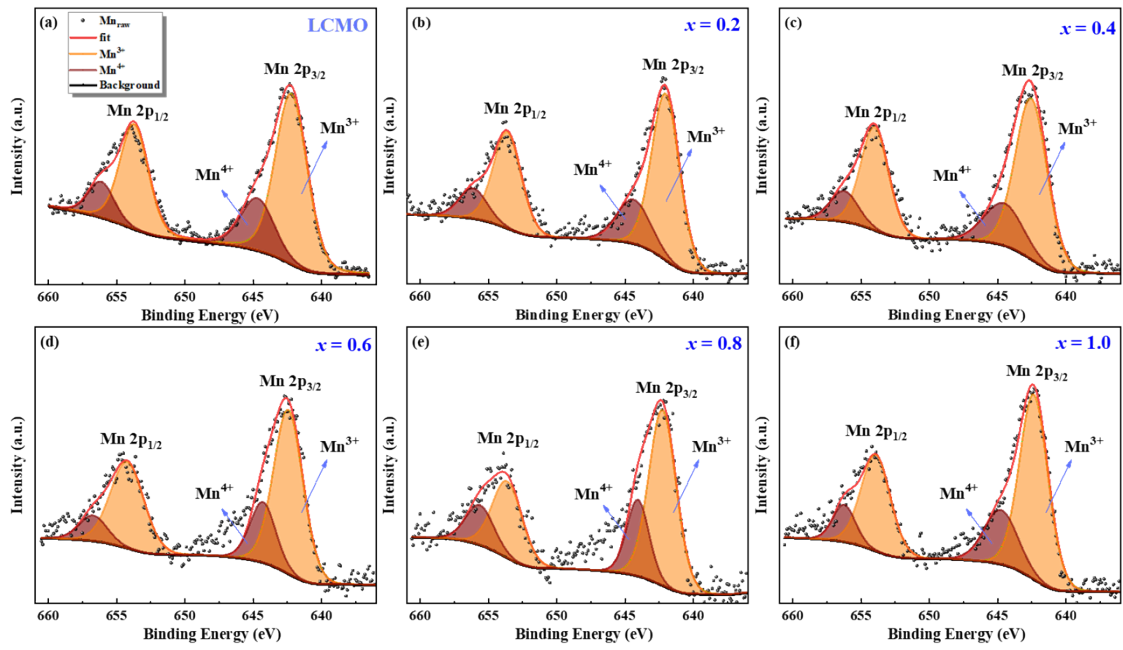


Fig. S6. Mn ion binding energy and fitting map of LS_xCMO samples (a) $x = 0$, (b) $x = 0.2$, (c) $x = 0.4$, (d) $x = 0.6$, (e) $x = 0.8$, (f) $x = 1.0$.

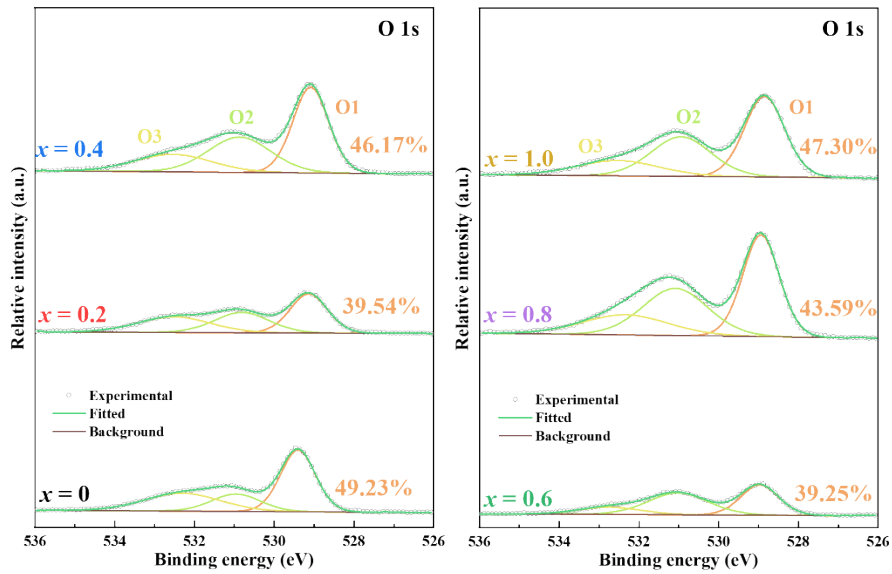


Fig. S7. Deconvoluted O-1s XPS spectra of La_{2-x}Sr_xCoMnO₆ ($x = 0 \sim 1.0$) ceramics.

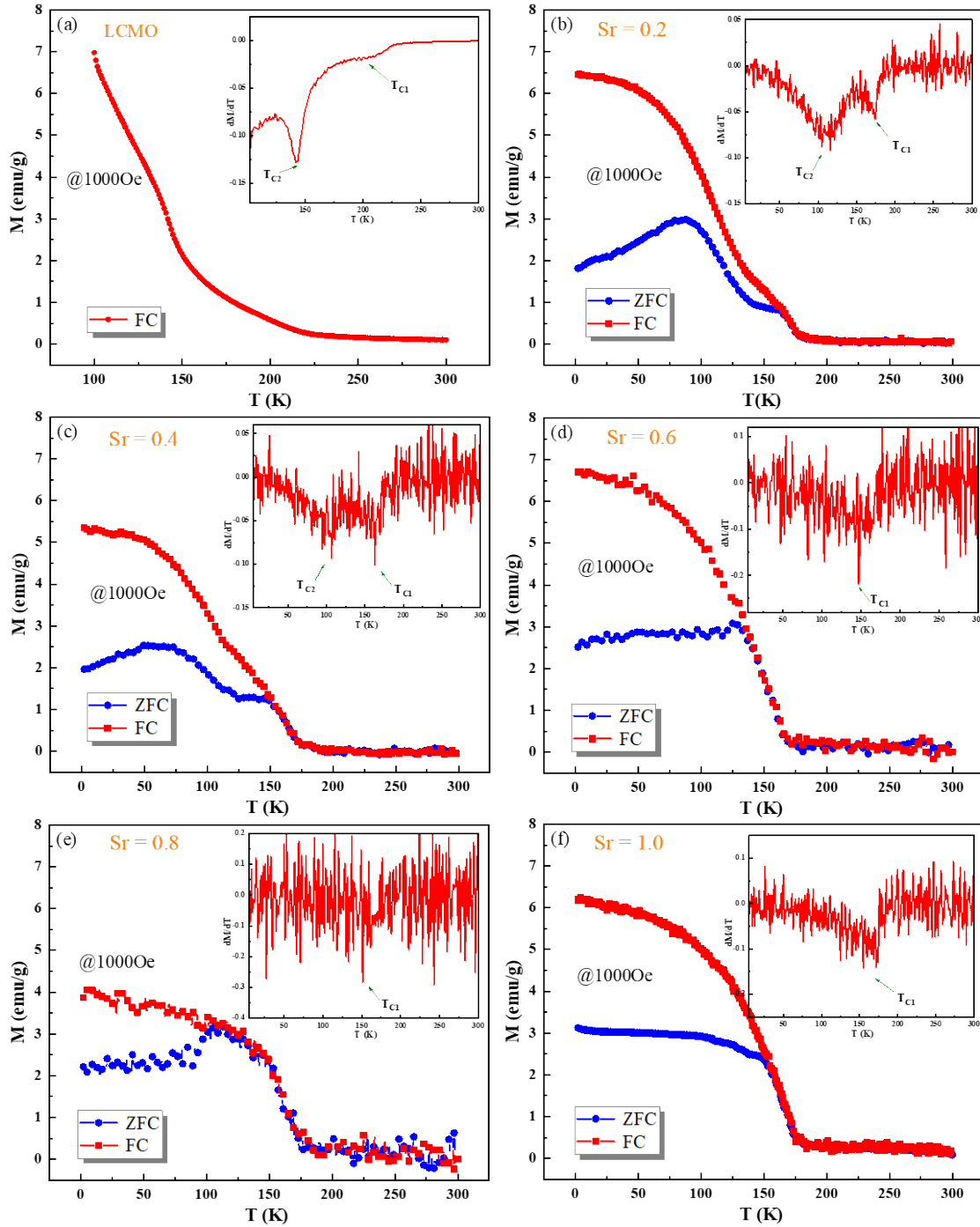


Fig. S8. M - T data under ZFC and FC modes for 1000 Oe field in the LS x CMO samples (a) $x = 0$, (b) $x = 0.2$, (c) $x = 0.4$, (d) $x = 0.6$, (e) $x = 0.8$, (f) $x = 1.0$, and the inset of their respective figures represents the first derivative of ZFC magnetization with temperature.